

# ABSENCE OF DWARF GALAXIES AT HIGH REDSHIFTS: EVIDENCE FROM A GALAXY GROUP

WILLIAM G. MATHEWS<sup>1</sup>, LAURA CHOMIUK<sup>1</sup>, FABRIZIO BRIGHENTI<sup>1,2</sup>, & DAVID A. BUOTE<sup>3</sup>

*Draft version September 4, 2018*

## ABSTRACT

The galaxy group NGC 5044 consists of a luminous giant elliptical galaxy surrounded by a cluster of  $\sim 160$  low luminosity and dwarf galaxies, mostly of early type. The cumulative projected radial distribution of dwarf galaxies in the NGC 5044 group, unlike distributions of more luminous galaxies in rich clusters, does not follow a projected dark matter (NFW) profile. A deficiency or absence of low luminosity galaxies is apparent in NGC 5044 within about 350 kpc. Most of the dwarf galaxies in NGC 5044 entered the virial radius at redshifts  $z \lesssim 2 - 3(a_f/0.25)$ , where  $a_f = 1/(1 + z_f)$  is the epoch of group formation, and very few entered during redshifts  $z \gtrsim 2 - 3(a_f/0.25)$ . The peculiar, non-NFW shape of the projected cumulative dwarf galaxy distribution in NGC 5044 within 350 kpc resembles the characteristic cumulative distribution of dark subhalos that are also known to be relatively young. Dynamical friction is unlikely to explain the apparent lack of group member galaxies at small radii in NGC 5044.

*Subject headings:* galaxies: elliptical and lenticular, CD – galaxies: dwarfs – clusters – groups – feedback

## 1. INTRODUCTION

The early evolution of dwarf galaxies is of interest because of the possible great antiquity of these galaxies and because they lie near the lowest mass scale for hierarchical assembly in which low mass galaxies merge to form normal galaxies of larger mass. Efforts to understand the evolution of these faint galaxies have been frustrated because of the difficulty of direct observation at cosmologically relevant redshifts. Theoretical models of the formation of dwarf galaxies are complicated by the poorly understood role of supernova feedback and cosmic photoionization that may limit star formation at certain redshifts. Finally, there is much consternation about N-body calculations that predict many more dwarf galaxies than are actually observed (Moore et al. 1999).

We describe here a simple means of determining the space density of dwarf galaxies in the early universe by observing their projected spatial distribution in galaxy groups. Of particular interest are galaxy groups, such as NGC 5044, that contain large numbers of dwarf galaxies and for which the virial mass is well known from X-ray observations. These groups are often dominated by a single, centrally-located luminous elliptical galaxy. Since the masses of dwarf galaxies are very small compared to the group virial mass, their dynamics are very similar to dark matter particles. As dark halos grow by accretion from the inside out, so does the spatial distribution of associated dwarf galaxies. Dwarf galaxies currently orbiting closest to the central elliptical galaxy must be among the oldest galaxies in the group.

It is therefore of considerable interest that the cumulative projected radial distribution of dwarf galaxies in the

NGC 5044 group does not follow the standard projected mass distribution of the dark matter halo. Instead, the number of dwarf galaxies per unit dark matter appears to be lower within a projected radius  $R \approx 350$  kpc. We show here that this central shortfall implies that dwarf galaxies were underabundant relative to the ambient dark matter at redshifts  $z \gtrsim 3$ . This cosmic variation of dwarf galaxy density is opposite to that recently proposed to explain the increasing number of dwarf galaxies in richer clusters.

## 2. OBSERVED GALAXIES IN NGC 5044

On first inspection, the central elliptical galaxy in the NGC 5044 group, with luminosity  $L_B = 4.5 \times 10^{10} L_{B,\odot}$ , completely dominates the optical image of the cluster. A closer look reveals a cluster of about 160 low-luminosity galaxies surrounding the central elliptical that extends out to 500 kpc and beyond (Ferguson & Sandage 1990; FS). At 33 Mpc (e.g. Tonry et al. 2001) the absolute magnitudes of the non-central galaxies range from  $M_B = -19$  to  $-13$ , i.e.  $2 \times 10^7 \lesssim L_B \lesssim 9 \times 10^9 L_{B,\odot}$ . About 80 percent of the non-central group members appear to be spheroidal or dE galaxies (FS). Most or all of these galaxies are dwarfs, depending on one's threshold for dwarf designation. Unfortunately, cluster membership has not yet been fully confirmed with radial velocity measurements, but we have removed several Ferguson-Sandage galaxies from the membership list – FS68, FS102, and FS137 – because their velocities differ by more than  $\pm 800$  km s<sup>-1</sup> from that of the central elliptical (NED, Garcia 1993). Nevertheless, the remarkably high space density of these galaxies and their symmetric distribution largely confirm their physical association with the central elliptical (NGC 5044). In any case, we assume here that most of the galax-

<sup>1</sup> University of California Observatories/Lick Observatory, Department of Astronomy and Astrophysics, University of California, Santa Cruz, CA 95064, mathews@ucolick.org

<sup>2</sup> Dipartimento di Astronomia, Università di Bologna, via Ranzani 1, Bologna 40127, Italy, brighenti@bo.astro.it

<sup>3</sup> University of California at Irvine, Dept. of Physics & Astronomy, 4129 Frederick Reines Hall, Irvine, CA 92697, buote@uci.edu

ies regarded as members or likely members by Ferguson & Sandage are indeed members.

Of particular interest is the radial distribution of the galaxies in NGC 5044. Carlberg, Yee & Ellingson (1997) and Biviano & Girardi (2003) have shown that the mean surface number density of galaxies in richer clusters closely follows the NFW profile expected for the underlying dark matter (Navarro, Frenk, & White 1997). The luminosities of the galaxies considered by Carlberg et al. are much larger than those found in NGC 5044. An NFW distribution for optical galaxies would be expected if galaxies entered the virial mass of the cluster evenly over time and suffered no significant radial migration by dynamical friction not also experienced by the dark matter.

Remarkably, the projected distribution of the low luminosity galaxies in NGC 5044 differs dramatically from an NFW profile. Instead of the NFW central peak, the satellite galaxies in NGC 5044 have a King-like core that extends to  $\sim 150$  kpc (Ferguson & Sandage 1990). This difference is apparent in Figure 1 where we compare the cumulative number of non-central galaxies as a function of projected radius  $R$  with an NFW mass surface density profile (Bartelmann 1996). The current virial mass and radius of NGC 5044,  $M_{v,o} \approx 4 \times 10^{13} M_{\odot}$  and  $r_{v,o} = 887$  kpc, are known from X-ray observations (Buote, Brighenti & Mathews 2004). In Figure 1 both distributions are normalized to agree at  $R = 350$  kpc. A Kolmogorov-Smirnov test applied within 350 kpc reveals that the observed cumulative galaxy distribution in NGC 5044 has a nearly vanishing likelihood of being consistent with the NFW profile. The normalization that we have chosen, forcing agreement at  $R = 350$  kpc, is reasonable because the two distributions then agree reasonably well in the range  $325 \lesssim R \lesssim 500$  kpc. For  $R \gtrsim 500$  kpc the number of identified galaxies falls below the NFW profile. We assume that this discrepancy is due to an incompleteness in identifying cluster members, but the projected radius where the incompleteness sets in could be somewhat smaller.

Galaxies that joined the NGC 5044 group at high redshift when the virial radius was smaller have orbits with maximum radial excursions near this virial radius. These galaxies spend most of their time orbiting near this same radius. As we show below, dynamical friction is relatively ineffective for dwarf galaxies. Therefore, the numerical shortfall of low luminosity galaxies in the core of NGC 5044 ( $R \lesssim 350$  kpc) suggests that proportionally fewer galaxies entered the virial radius at high redshift. In the following section we develop a simple dynamical model for the evolution of orbiting galaxies in NGC 5044 that can be used to quantify the relative absence of low-luminosity galaxies in the early universe.

The shallow projected distribution of galaxies around NGC 5044 may not be unique. Klypin et al. (1999) note the lack of dwarfs in low density regions like the Local Group. Smith, Martinez & Graham (2003) find that the radial surface density of dwarf galaxies varies as  $R^{-0.6 \pm 0.2}$  around a sample of isolated elliptical galaxies; this is flatter than NFW except for the innermost regions. Madore, Freedman & Bothun (2004) also find that the surface density of satellite galaxies near individual ellipticals declines as  $R^{-0.5}$ , while earlier studies by Vader & Sandage (1991) and Lorrimer et al (1994) indicate a

steeper decline,  $R^{-1}$ . Dwarf galaxies in the Fornax cluster have a shallower cumulative radial distribution than the giant galaxies (Drinkwater et al. 2001). Very recently, Pracy et al. (2004) have discovered a relative deficiency of dwarf galaxies in the central regions of the cluster Abell 2218. The physical scale of the region of dwarf depletion,  $\sim 400$  kpc, is very similar to that in NGC 5044. In Abell 2218 the ratio of the projected numbers of dwarf to giant galaxies decreases with increasing surface density of giant galaxies, as noted by Phillipps et al. (1998).

### 3. DYNAMICAL MODEL FOR SATELLITE GALAXIES

We estimate the expected radial distribution of galaxies in NGC 5044 by following the orbits of cluster member galaxies in the time-dependent dark matter potential of the cluster. The galaxies are regarded as test particles without structure. Newly accreted galaxies are assumed to arrive at the virial radius having fallen from the local turnaround radius. The orbits are not entirely radial since galaxies acquire some angular momentum due to attractions by neighboring inhomogeneities. After entering the virial radius, galaxies orbit until the present time when their projected distances from the center of the cluster can be compared with the radial distribution observed in NGC 5044.

The first model we consider is a galaxy cluster in which the local space density of galaxies is proportional to that of the dark matter, as if a fixed fraction of baryons formed into low-luminosity galaxies at a very early time. In this case the dynamics of dark matter and surviving dwarf galaxies are identical. Dark matter halos grow from the inside out by radial accumulation and accretion by mergers. The mass assembly histories of dark halos are universal and scale invariant, apart from differences in formation times. From studies of N-body simulations in a  $\Lambda$ CDM cosmology it has been determined that the mass of virialized dark matter increases with decreasing redshift  $z$  to its current value  $M_{v,o}$  according to

$$M_v = M_{v,o} e^{-2a_f z} \quad (1)$$

where  $a_f = 1/(1 + z_f)$  defines the halo ‘‘formation’’ time (Wechsler et al. 2002). We adopt  $a_f = 0.25$  here, but the redshifts we derive can be easily scaled to other values of  $a_f$  by keeping  $a_f z$  constant. At every time or redshift the radial profile of dark matter is described by an NFW profile (Navarro, Frenk & White 1997) that is parameterized by the virial mass  $M_v$  and the concentration

$$c(M_v, z) = 450(M_v/M_{\odot})^{-0.1283} (1 + z)^{-1} \quad (2)$$

(Wechsler et al. 2002), based on a  $\Lambda$ CDM cosmology with  $\Omega_o = 0.3$ ,  $\Omega_{\Lambda,o} = 0.7$  and  $H_o = 70$  km s $^{-1}$  Mpc $^{-1}$ .

For the idealized circumstance in which dwarf galaxies observed in clusters today all formed at some very early time, they enter the virialized halo at the same rate as the dark matter. With this simple model the virialized mass  $M_{v,i}$  when the  $i$ th galaxy first entered the virialized halo can be found from

$$M_{v,i} = \mathcal{R} M_{v,o} \quad (3)$$

where  $0 \leq \mathcal{R} \leq 1$  is a random number. The redshift  $z_i$  at entry can be found from Equation (1) and the corresponding cosmic time  $t_i(z_i)$  is determined by the  $\Lambda$ CDM cosmology.

The virial radius at time  $t_i$  is

$$r_{v,i} = \left( \frac{3M_{v,i}}{4\pi\Delta_i\rho_{c,i}} \right)^{1/3} \quad (4)$$

where  $\rho_{c,i} = 3H_i^2/8\pi G$  is the critical density and the appropriate  $\Lambda$ CDM overdensity factor is

$$\Delta_i = 18\pi^2 + (\Omega(z_i) - 1)[82 - 39(\Omega(z_i) - 1)]. \quad (5)$$

The velocity of galaxies arriving at  $r_{v,i}$ ,

$$u_{v,i} = (GM_{v,i}/r_{v,i})^{1/2}, \quad (6)$$

is the freefall velocity from the turnaround radius  $r_t = 2r_v$ , and we ignore the small dark energy term, i.e.  $\Lambda r_v^2 \ll GM_v/r_v$ .

If the dark matter distribution were perfectly smooth, the orbits of dark matter particles and galaxies would be perfectly radial. In this case the dark matter halos would be more centrally concentrated than the NFW profile (Bertschinger 1985). However, because of inhomogeneities in the dark matter distribution, random velocities are induced by mutual gravitational attraction. Consequently, galaxies arriving at the virial radius have acquired some angular momentum that is essential in determining the NFW profile. Considering the importance of this effect and the large number of available N-body dark matter calculations, it is surprising that the angular momentum distribution has not been discussed in full detail. We are fortunate, however, that Tormen (1997) and Ghigna et al. (1998) have plotted the distribution of circularity  $\epsilon = J/J_c$  at  $r_v$  where  $J$  is the specific angular momentum of dark matter particles and  $J_c = u_v r_v$  is the maximum angular momentum at the virial radius;  $\epsilon = 1$  for circular orbits and  $\epsilon = 0$  for radial orbits.

Based on these results we model the probability density for circularity  $p'(\epsilon) = dp/d\epsilon$  with a third order polynomial, subject to the constraints that  $p'(0) = p'(1) = 0$  and normalized so the integral of  $p'(\epsilon)$  from 0 to 1 is unity. The resulting distribution is

$$p'(\epsilon) = a\epsilon^3 - (1.5a+6)\epsilon^2 + (0.5a+6)\epsilon \equiv A\epsilon^3 - B\epsilon^2 + C\epsilon \quad (7)$$

where

$$a = 60(1 - 2\langle\epsilon\rangle) \quad (8)$$

and  $\langle\epsilon\rangle$  is the mean circularity. The results of Tormen suggest that  $\langle\epsilon\rangle \approx 0.5$ , for which  $p'(\epsilon)$  becomes a symmetric quadratic. However, the circularity distribution of Ghigna et al. is skewed toward larger  $\epsilon$  so we also entertain this possibility. Random values of  $\epsilon$  can be found from

$$\mathcal{R} = \int_0^\epsilon p'(\epsilon)d\epsilon = (A/4)\epsilon^4 - (B/3)\epsilon^3 + (C/2)\epsilon^2. \quad (9)$$

All galaxies have velocity  $u_{v,i}$  given by Equation (6) when they first enter the virial radius; the angular momentum  $J = J_c\epsilon$  is used to allocate the direction of this velocity.

The galaxy orbits are found by solving

$$\frac{d\mathbf{r}}{dt} = \mathbf{u} \quad \text{and} \quad \frac{d\mathbf{u}}{dt} = -\frac{GM(r)\mathbf{r}}{r^2}. \quad (10)$$

Within the virial radius the NFW mass distribution is

$$M(r) = M_v(t) \frac{f(y)}{f(c)} \quad (11)$$

where  $f(y) = \ln(1+y) - y/(1+y)$  and  $y = cr/r_v$ . At higher redshifts, when the virial mass grows more rapidly, most entering galaxies orbit entirely within the increasing

virial radius. At lower redshifts, however, some galaxies move briefly outside  $r_v(t)$ . In this case we use the exterior dark matter mass density distribution corresponding to the density derived by Barkana (2003)

$$\rho = \rho_{v+}(r/r_v)^{-1.3} \quad r > r_v. \quad (12)$$

The density just beyond the virial radius is found from

$$\rho_{v+} = \frac{1}{4\pi r_v^2 u_v} \frac{dM_v}{dt}. \quad (13)$$

Galactic orbits are computed from the time  $t_{v,i}$  when they first reach the virial radius until the current time  $t_n = 13.5$  Gyrs. At time  $t_n$  the radius of each galaxy  $r_i$  is randomly projected on the plane of the sky,

$$R_i = [1 - (2\mathcal{R} - 1)^2]^{1/2} r_i. \quad (14)$$

#### 4. RESULTS

The thin lines in Figure 1 show the results of two dynamical models calculated as described in the previous section. For these models, and those discussed below, the Monte Carlo simulations are continued until 1210 galaxies occupy the region  $R < 350$  kpc at time  $t_n$ . This is ten times the observed number in this region. The total number of orbits required to achieve this limit is typically almost twice as large. The computed projected radial distributions are normalized to agree with the NFW mass distribution at a projected radius  $R = 350$  kpc. The light curve (actually a histogram) in Figure 1 labeled  $\langle\epsilon\rangle = 0.5$  was computed with this constant mean circularity for all orbits during the evolution of the dark halo. Since Equation (3) requires that the arrival of galaxies into the virialized dark halo is identical to that of the dark matter, their cumulative distribution should be identical to the NFW profile. The agreement in Figure 1 is seen to be very good indeed, particularly considering the simplicity of our model. The mean assembly history for the dark halo implicitly allows for all past halo-halo mergers. When two halos merge, orbiting bound galaxies also merge in a manner that approximately conserves the orbital phase space density, and this maintains their relative mean locations in the merged dark halo potential.

As the projected radius  $R$  approaches the current virial radius of NGC 5044,  $r_{v,o} = 887$  kpc, the number of galaxies in the  $\langle\epsilon\rangle = 0.5$  calculation in Figure 1 falls about 10 percent below the NFW expectation. This deviation probably occurs because there are too many ( $\sim 100$ ) galaxies at radii  $r > r_{v,o}$  at time  $t_n$ . This discrepancy is insensitive to the value of the mean circularity  $\langle\epsilon\rangle$ , i.e. nearly identical results are obtained for  $\langle\epsilon\rangle = 0.3$  or 0.7. However, if  $\langle\epsilon\rangle$  is assumed to increase steadily with the virialized mass,  $\langle\epsilon\rangle = M_v/M_{v,o}$ , the discrepancy is somewhat reduced. This result with time-varying  $\langle\epsilon\rangle$ , illustrated in Figure 1 as “var  $\langle\epsilon\rangle$ ”, has no independent dynamical motivation. Other small procedural changes, perhaps in Equation (6), could be considered to reduce the discrepancy near the virial radius, but we have not explored this since the results shown in Figure 1 are certainly good enough for the region of most interest,  $R \lesssim 500$  kpc.

Figure 2 shows the average halo entry redshift  $\langle z_i \rangle$  for galaxies in annular bins at time  $t_n$  for the two dynamical models shown in Figure 1 (open and filled circles). The

redshift dispersions are mostly intrinsic, and do not simply reflect the finite number of orbiting galaxies in each projected bin. As expected, the mean arrival redshift rises sharply toward the center of the cluster. Provided the space density of low luminosity galaxies is proportional to the dark matter density at all redshifts, as imposed by Equation (3), the increase in mean redshift with decreasing projected radius  $R$  is robust, essentially independent of the value or time variation of  $\langle\epsilon\rangle$ . In the following we assume  $\langle\epsilon\rangle = 0.5$ .

The sense of the discrepancy in Figure 1 between the cumulative number of galaxies in NGC 5044 and the NFW profile indicates that the space density of low luminosity galaxies relative to dark matter was lower at higher redshifts. This discrepancy can be incorporated into our models if we relax the assumption of uniform, early galaxy formation (Equation 3). We shall consider only models in which the space density of dwarf galaxies is constant or increases monotonically with time.

Suppose for example that the satellite galaxies in NGC 5044 began to form at a redshift  $z_c$  when the halo mass was  $M_c$  and increased as a power law afterward. In this case the probability density for arrival of a galaxy into the virialized halo is  $p'(M_v) = p_o(M_v - M_c)^q$ . When  $p'(M_v)$  is properly normalized, the virial mass at which a random galaxy enters the halo is

$$M_{v,i} = M_c + (M_{v,o} - M_c)\mathcal{R}^{1/1+q} \quad (15)$$

where  $\mathcal{R}$  is a random number. This reduces to Equation (3) when  $M_c = q = 0$ .

Figure 3 shows three evolutionary sequences in which galaxies are assumed to begin forming at the earliest possible epoch ( $M_c = 0$ ) and increase in number afterward according to a power law,  $p' \propto M_v^q$ . Of the three possible powerlaws,  $q = 2$  is seen to follow best the observed number of galaxies in NGC 5044 at small  $R$ . As before, all solutions are normalized at  $R = 350$  kpc. Solutions with  $q = 0.75$  ( $q = 3.5$ ) produce too many (few) galaxies within 350 kpc, but the  $q = 2$  histogram follows the observed histogram almost perfectly in this region. Nevertheless, none of these pure powerlaw models produce the slope change at  $\sim 350$  kpc that is apparent in the observations. If the  $q = 2$  solution is correct, the observations would have to begin to be incomplete just where this slope change occurs. This is possible but implausible. It seems unlikely that Ferguson & Sandage would have missed identifying  $\sim 50$  member galaxies in the region  $350 \lesssim R \lesssim 500$  kpc. The total number of galaxies expected inside the projected virial radius 887 kpc at  $t_n$  is 237, 305 and 352 for orbits with  $q = 0.75, 2$  and  $3.5$  respectively.

In Figure 4 we plot a better model in which no small galaxies form before redshift  $z_c = 3.32$  ( $M_c = 0.19M_{v,o}$ ), followed by a powerlaw rise with  $q = 0.1$ . This solution fits the observations almost perfectly in  $R \lesssim 350$  kpc and continues to increase thereafter in approximate proportion to the dark matter. The mean binned redshifts for this dynamical model, plotted as open squares in Figure 2, shows that the observations are consistent with very few galaxies in NGC 5044 having accretion redshifts  $\gtrsim 2$ .

Since the powerlaw rise with  $q = 0.1 < 1$  is abrupt, we also considered a variety of step function models for  $p'(M_v)$ . In these models  $q \rightarrow 0$  and the virial mass at the

time of galaxy arrival is

$$M_{v,i} = M_c + \mathcal{R}(M_{v,o} - M_c) \quad (16)$$

where the halo mass  $M_c$  corresponds to redshift  $z_c = -2 \ln(M_c/M_{v,o})$ . The step function solution with  $z_c = 2.77$  shown in Figure 4 also agrees very well with the NGC 5044 observations, assuming some small incompleteness at  $R \gtrsim 350$  kpc and few foreground or background interlopers.

As a final alternative model we show in Figure 4 a solution in which the probability density  $p'(M_v)$  rises initially as a power law until  $M_v = M_*$  and is constant thereafter. For models of this type the mass at which galaxies arrive in the halo is given by

$$M_{v,i} = M_*(\mathcal{R}/\mathcal{R}_*)^{1/p+1} \quad (17)$$

if

$$\mathcal{R} < \mathcal{R}_* \equiv [1 + (p+1)(M_{v,o} - M_*)/M_*]^{-1} \quad (18)$$

and

$$M_{v,i} = M_*[1 - (1 - \mathcal{R}/\mathcal{R}_*)/(p+1)] \quad (19)$$

if  $\mathcal{R} > \mathcal{R}_*$ . A solution with  $p = 2.5$  and  $M_* = 0.4M_{v,o}$  ( $z_* = 1.83$ ) is shown in Figure 4. This solution also fits the NGC 5044 data remarkably well within 350 kpc and corresponds to a modest incompleteness in the observed number of galaxies at larger radii.

Overall, we are struck by the ease at which our various dynamical models having a relative absence of high redshift dwarf galaxies fit the histogram observed by FS within  $\sim 350$  kpc. This excellent agreement gives us confidence that the FS data are reasonably complete in the dense central region of NGC 5044 and that the number of dwarf galaxies per unit dark matter is indeed much lower for entry redshifts  $z \gtrsim 2.5/(a_f/0.25)$  than afterwards.

In addition, we note that the cumulative radial projected distributions of dark subhalos in N-body calculations (e.g. de Lucia, G. et al. 2004; Gao et al 2004) are also shallower than that of the underlying dark halo and have histograms very similar to the observed cumulative number of dwarfs in NGC 5044. This is reasonable since subhalos are continuously destroyed, so surviving subhalos are relatively young (Gao et al. 2004). However, the evolution of dark subhalos and dwarf galaxies differs because the subhalos are known to be disrupted and dissolved by tidal forces and dynamical friction.

## 5. DYNAMICAL FRICTION

Can the scarcity of high redshift dE galaxies in the NGC 5044 group be understood as a depletion of central galaxies by dynamical friction? The answer is not so obvious since dynamical friction increases with the orbiting mass and the initial dark mass associated with each dwarf galaxy may have been rather large. However, if the central region of NGC 5044 is depopulated by dynamical friction, it may be repopulated by galaxies that decay by dynamical friction from initially larger orbits. To address this question we have made a series of orbital calculations including an additional dynamical friction term in the second Equation (10),

$$\left(\frac{du}{dt}\right)_{df} = -\mathbf{u} \cdot 4\pi \ln \Lambda G^2 M \rho u^{-3} [\text{erf}(X) - \frac{2}{\pi^{1/2}} X e^{-X^2}]. \quad (20)$$

(Chandrasekhar 1943). Here  $\rho(r, t)$  is the local density of halo dark matter,  $u = |\mathbf{u}|$  is the galactic velocity,  $X = u/2^{1/2}\sigma$  and  $\sigma(r, t)$  is the mean velocity dispersion of dark matter particles in the NGC 5044 halo. According to Hoefl, Mücke & Gottlöber (2004), the dispersion velocity of dark matter is approximately isotropic with maximum value  $\sigma_m = 1.25 \pm 0.20(GM_v/r_v)^{1/2}$  and radial distribution  $\sigma(r)/\sigma_m = [2/(\xi^{-0.5} + \xi^{0.6})]^{1/2}$  where  $\xi = 2y$  and  $y = cr/r_v$ . We choose  $\ln \Lambda = 3$  as suggested by Zhang et al. (2002) and others. Because of the high density and compact nature of dwarf galaxies, we approximate the orbiting galaxies with point masses.

In selecting galaxies we assume random halo entry redshifts given by Equation (3). The mass of the  $i$ th galaxy is  $M_i = \Upsilon_B L_{B,i}$  where  $\Upsilon_B$  is an adjustable mass to light ratio and the galactic luminosity is randomly selected from the power law part of the Schechter luminosity function  $dN/dL_b \propto L_B^{-1.2}$  (which is satisfied by NGC 5044),

$$L_{B,i} = [L_1^{-0.2} - \mathcal{R}(L_1^{-0.2} - L_2^{-0.2})]^{-5}. \quad (21)$$

Here  $L_1 = 2 \times 10^7 L_{B,\odot}$  and  $L_2 = 9.2 \times 10^9 L_{B,\odot}$  span the range of non-central galaxies in NGC 5044.

The ratio of stellar to dark mass in dwarf galaxies is uncertain since mass to light ratios  $\Upsilon_B$  can only be observed in the central region containing luminous stars. Observations of several dE galaxies by Geha et al. (2002) indicate  $3 \lesssim \Upsilon_B \lesssim 6$ , but the total value could be higher, depending on the severity of tidal truncation. Consequently, we computed galactic orbits using the friction term (20) with values of  $\Upsilon_B = 0 - 100$ . Circularities were determined by Equation (9) assuming  $\langle \epsilon \rangle = 0.5$ .

For all values of  $\Upsilon_B$  considered the cumulative number of galaxies at time  $t_n$  closely follows the NFW profile (normalized at  $R = 350$  kpc) and resembles very closely the  $\langle \epsilon \rangle = 0.5$  solution in Figure 1. For  $\Upsilon_B = 4$  only  $\sim 2$  percent of the dwarf galaxies merge into the central E galaxy, but this increases to 4 or 15 percent if  $\Upsilon_B = 10$  or 100 respectively. Even with these very large  $\Upsilon_B$ , the loss of galaxies by inward migration and central mergers does not appreciably alter their radial distribution at time  $t_n$ . For all  $\Upsilon_B$  considered the redshift distribution of surviving galaxies at  $t_n$  is essentially the same as that shown in Figure 2 for the  $\langle \epsilon \rangle = 0.5$  solution without dynamical friction.

However, when  $\Upsilon_B \gtrsim 30$  we find that the average luminosity  $\langle L_B \rangle$  of surviving galaxies decreases. Since the drag force is proportional to  $M d\mathbf{u}/dt \propto M^2 \propto (\Upsilon_B L_B)^2$ , the onset of dynamical friction is rather abrupt as the mass or  $L_B$  of orbiting galaxies increases. This may explain why the luminosity distribution of low-luminosity galaxies observed in NGC 5044 cuts off rather abruptly at  $L_B \approx L_2$ . In orbital calculations using Equation (3) and including dynamical friction, the average luminosity of surviving satellite galaxies  $\langle L_B \rangle$  drops by 10 or 20 percent if  $\Upsilon_B = 15$  or 30 respectively. For  $\Upsilon_B = 65$ ,  $\langle L_B \rangle$  is only half as large as the average galaxy observed in  $L_1 < L_B < L_2$  because a larger fraction of these more massive galaxies have computed orbits that merge at the center under dynamical friction. We conclude that the mass to light ratios of the (possibly tidally truncated) low luminosity galaxies in NGC 5044 cannot be much larger than  $\sim 30$ . Summarizing, (1) for reasonable dwarf galaxy mass to light ratios  $\Upsilon_B$  dynamical friction is not very important, and (2) the

main effect of increasing  $\Upsilon_B$  above  $\sim 30$  is to deplete the more luminous dwarfs relative to those observed in NGC 5044.

## 6. DISCUSSION AND CONCLUSIONS

We emphasize the distinction between the evolution of group member galaxies and dark matter subhalos, which has been a source of confusion in recent discussions. Subhalos are formed by dark matter inhomogeneities that are accreted into the main halo. As these subhalos undergo tidal disruption and dynamical friction, they melt into the main cluster halo so surviving subhalos at any time are comparatively young. However, the dense baryonic galactic cores in subhalos are very deeply bound and are much more resistant to dynamical disruption than the surrounding subhalos. The dynamical distinction between ephemeral subhalos and long-lived galactic cores has been discussed for massive clusters by Gao et al. (2004) who use N-body and semi-analytic methods to reproduce both the shallow, non-NFW cumulative distribution of dark subhalos and the nearly NFW distribution of surviving galaxies (Carlberg, Yee & Ellingson 1997). Within the resolution limit of the calculation of Gao et al., the surviving galaxies typically have lost their extended dark halos by tidal disruption and this is likely to be true in NGC 5044 as well.

We also emphasize that the final galactic distributions calculated here refer only to cluster member galaxies that survive today. Many more massive galaxies that did not survive (and are therefore not included in most orbits considered here) merged to form the giant elliptical at the center of NGC 5044. An integral over a Schechter luminosity distribution from the most luminous orbiting galaxy in NGC 5044  $L_B = L_2$  to infinite  $L_B$  is comparable to the luminosity of the central galaxy (Jones, Ponman & Forbes 2000). This is consistent with the notion that the central elliptical was formed by mergers of all first generation galaxies with  $L_B > L_2$ .

The relative absence of dwarf galaxies that entered the virial radius of NGC 5044 at high redshifts is exactly opposite to the behavior that has been proposed to explain the excess of dwarf galaxies in rich clusters (Klypin et al. 1999; Bullock, Kravsov & Weinberg 2000; Trentham, Tully & Verheijen 2001; Tully et al. 2002; Tassis et al. 2003). Tully et al. (2002) argue, for example, that the relative lack of dwarf galaxies in the Ursa Major cluster ( $M_v = 4 \times 10^{13} M_\odot$ ) relative to the Virgo cluster ( $M_v = 8 \times 10^{13} M_\odot$ ) can be understood if most of the dwarfs in Ursa Major formed after cosmic reionization at redshift  $z_{ion} \gtrsim 6$  when the heated baryonic gas was less able to form stars. Late forming dwarfs also have lower dark matter (and gas) densities, further suppressing star formation. Conversely, it is argued that the Virgo cluster is much older and its (more numerous) dwarfs formed before reionization.

Evidently, dwarf galaxy formation and the faint end of the galaxy luminosity function may vary with space and time due to environmental influences. The relatively small number of surviving dwarf galaxies that entered the virial radius of NGC 5044 during redshifts  $6 \gtrsim z \gtrsim 2-3$  could be explained if stars were unable to form in small galaxies until  $z \sim 2-3$ . If the dark matter potential in low mass halos is sufficiently shallow, heating by early supernova feedback

or cosmic ionizing radiation may have kept the baryonic gas from cooling into stars. If no gas accumulated in or near low mass dark halos prior to redshift  $z \sim 2 - 3$ , only the dark halos of dwarf galaxies entered the virial radius of NGC 5044. To explain the existence of dwarf galaxies in NGC 5044 at smaller redshifts, it must be assumed that some baryonic gas eventually accreted into these halos and formed into the stars observed today. This scenario is possible, but unlikely. According to Susa & Umemura (2004), star formation in dwarfs with virial masses greater than  $\sim 10^8 M_\odot$  is unaffected by cosmic UV heating. For typical stellar mass to light ratios  $\Upsilon_{B,*} \sim 5$ , the stellar masses of the NGC 5044 dwarfs all exceed  $\sim 10^8 M_\odot$  and their original virial masses were  $\sim 10$  times larger. Therefore star formation in the dwarfs of NGC 5044 may be impaired but not completely shut down by cosmic UV heating. This is consistent with observations of nearby dwarf galaxies, many of them less massive than those in NGC 5044, that show no evidence that the star formation rate changed either at the epoch of reionization or at redshifts of  $\sim 2 - 3$  (Grebel & Gallagher 2004)

The apparent deficiency of high redshift dwarf galaxies in NGC 5044 can also be understood if these galaxies retained most of their gas at all relevant redshifts, provided very few baryons in these galaxies formed into stars before  $z \sim 2 - 3$ , as implied by the slow and sustained star formation in many well-observed local dwarf galaxies (e.g. Grebel & Gallagher 2004). Star formation in gas-rich dwarfs could be reduced either by proximity to NCC 5044 or by gas removal after the dwarf entered the virial radius of NGC 5044. Suppose for example that some disturbing process occurred during formation of the central galaxy (NGC 5044) – such as UV emission, outflowing winds, AGN activity etc. – that suppressed star formation in nearby dwarf galaxies. A necessary condition for this scenario is that the central formation starburst of NGC 5044 preceded the formation of most of the stars in the surrounding system of dwarf galaxies. As discussed already, even the least massive of the dwarfs identified in NGC 5044 is massive enough to retain ionized gas at  $\sim 10^4$  K, but gas heated to this temperature in gas-rich dwarf galaxies may expand sufficiently in the dwarf potential to greatly increase the efficiency of ram-pressure stripping after the galaxies entered the virialized hot gas in the NGC 5044 group. In this case the stellar component of high redshift dwarfs in NGC 5044 would be optically faint. One possible difficulty with this scenario is that the redshift range in Figure 2 corresponding to the reduced numbers of dwarfs,  $2 - 3 \lesssim z \lesssim 6$ , corresponds to almost 2 Gyrs and it is unlikely that an ionizing starburst (or AGN activity) can be maintained for this length of time. If the gas in dwarf galaxies is cooler than  $\sim 10^4$  K, it is unclear if it can be ram-stripped by the hot gas in NGC 5044.

Alternatively, could two-body interactions with larger galaxies, dark galaxies or subhalos at early times have scattered the orbits of dwarf galaxies originally near the center to larger radii in the NGC 5044 group? Probably not. Normal two-body galactic interactions are strongly masked by the large background dark matter density in NGC 5044 that dominates the force on each dwarf galaxy. For example, the concentrated baryonic mass of the central massive galaxy in this group is overwhelmed by the

ambient NFW dark mass beyond a radius of only 20 kpc. If galaxies are inefficient orbital scatterers, perhaps the softer potentials of massive dark subhalos within  $r \sim 350$  kpc in NGC 5044 strongly perturbed the orbits of dwarfs near the center. Unfortunately, subhalo perturbations are not likely to be effective since (1) X-ray observations and detailed N-body calculations verify that the dark matter orbiting in the central region of NGC 5044 is not selectively depleted in this way and (2) normal galaxies in the corresponding central regions of rich clusters are not scattered outward by dark subhalos. This is verified by the galaxy plus subhalo simulations of Gao et al. (2004) and by direct observation (Carlberg et al. 1997). The NFW distribution of luminous galaxies in rich clusters can be understood if these galaxies formed well in advance of the cluster potential.

We appeal to observers to study NGC 5044 and other similar groups in more detail. Group membership, particularly at large radii, must be confirmed with accurate radial velocities. Measured orbital velocities must also support the relative absence of dwarf galaxies at small radii. Group memberships should be determined out to the virial radius and beyond. If our interpretation of the incompleteness of the Ferguson-Sandage data is correct, another 50-100 members in NGC 5044 remain to be discovered in  $400 \lesssim R \lesssim 900$  kpc (Figure 1). If possible, estimates of the stellar ages in dwarfs as a function of projected radius could constrain our argument for a relative deficiency of old dwarfs having accretion redshifts  $6 \lesssim z \lesssim 2 - 3$ . An extension of group membership to dwarf galaxies of even lower luminosity could also be useful.

Our main conclusions are: (1) The cumulative projected radial distribution of dwarf galaxies in the NGC 5044 group does not follow a projected NFW profile, unlike observed distributions of more luminous galaxies in rich clusters. (2) Inside about 350 kpc in NGC 5044 there is a deficiency or absence of low luminosity galaxies relative to the NFW profile. (3) Most of the dwarf galaxies in this inner region of NGC 5044 that would have entered the virial radius at redshifts  $z/(a_f/0.25) \gtrsim 2 - 3$  are largely absent; most of the surviving dwarf galaxies in NGC 5044 first passed through the virial radius at redshifts  $z \lesssim 2 - 3(a_f/0.25)$ , where  $a_f = 1/(1 + z_f)$  is the epoch of group formation. (4) The peculiar, non-NFW shape of the depleted projected cumulative dwarf galaxy distribution in NGC 5044 within 350 kpc resembles the characteristic cumulative distribution of dark subhalos that are also known to be relatively young. (5) Dynamical friction is an unlikely explanation for the apparent lack of group member galaxies at small radii in NGC 5044. (6) The mass to light ratio  $\Upsilon_B$  of dwarf galaxies in NGC 5044 is unlikely to exceed  $\sim 30$  since otherwise the more luminous observed dwarf galaxies would have been lost by dynamical friction. (7) Our finding that dE galaxies did not appear until moderate redshifts is qualitatively consistent with the low mean stellar age of  $\sim 5$  Gyrs observed in dE galaxies (Geha et al 2002), i. e. many or most dwarf galaxies are younger than typical giant elliptical galaxies.

Studies of the evolution of hot gas in elliptical galaxies at UC Santa Cruz are supported by NASA grants NAG

5-8409 & ATP02-0122-0079 and NSF grants AST-9802994 & AST-0098351 for which we are very grateful.

#### REFERENCES

- Barkana, R. 2003, MNRAS (submitted) (astro-ph/0212458)  
 Bartelmann, M. 1996, A&A, 313, 697  
 Bertschinger, E. 1985, ApJS, 58, 39  
 Buote, D. A., Brighenti, F. & Mathews, W. G. 2004, ApJ, 607, L91  
 Biviano, A. & Girardi, M. 2003, ApJ, 585, 205  
 Bullock, J. S., Kravtsov, A. V., & Weinberg, D. H. 2000, ApJ, 539, 517  
 Carlberg, R. G., Yee, H. K. C. & Ellingson, E. 1997, ApJ, 478, 462  
 Chandrasekhar, S. 1943, ApJ, 97, 251 ApJ, 525, 720  
 de Lucia, G. et al. 2004, MNRAS, 348, 333  
 Drinkwater, M. J., Gregg, M. D., Holman, B. A., & Brown, M. J. I. 2001, MNRAS, 326, 1076  
 Ferguson, H. C. & Sandage, A. 1990, AJ, 100, 1  
 Gao, L., de Lucia, G., White, S. D. M. & Jenkins, A. 2004, MNRAS (submitted) (astro-ph/0405010)  
 Garcia, A. M. 1993, A&AS, 100, 47  
 Geha, M., Guhathakurta, P. & van der Marel, R. P. 2002, AJ, 124, 3073  
 Ghigna, S., Moore, B., Governato, F., Lake, G., Quinn, T. & Stadel, J. 1998, MNRAS, 300, 146  
 Grebel, E. K. & Gallagher, III, J. S. 2004, ApJ Letters (in press) (astro-ph/0407117)  
 Hoeft, M., Mücke, J. P. & Gottlöber, S. 2004, ApJ, 602, 162  
 Jones, L. R., Ponman, T. J. & Forbes, D. A. 2000, MNRAS, 312, 139  
 Klypin, A., Kravtsov, A., Valenzuela, O. & Prada, F. 1999, ApJ, 522, 82 2004, ApJ, (submitted) (astro-ph/0401088)  
 Lorrimer, S. J. et al. 1994, MNRAS, 269, 696  
 Madore, B. F., Freedman, W. L. & Bothun, G. D. 2004, ApJ, 607, 810  
 Moore, B., Ghigna, S., Governato, F., Lake, G., Quinn, T., Stadel, J. & Tozzi, P. 1999, ApJ, 524, L19 ApJ, 514, 133  
 Navarro, J. F., Frenk, C. S. & White, S. D. M. 1997, MNRAS, 490, 493  
 Phillipps, S., Driver, S. P., Couch, W. J., & Smith, R. M. 1998, ApJ, 489, L119  
 Pracy, M. B., De Propris, R., Driver, S. P., Couch, W. J. & Nulsen, P. E. J. 2004, MNRAS (in press) (astro-ph/0405421)  
 Smith, R. M., Martinez, V. J. & Graham, M. J. 2003, ApJ, submitted (astro-ph/0311599)  
 Susa, H. & Umemura, M. 2004, ApJ, 601, L5 2003, MNRAS, 341, 434  
 Tassis, K., Abel, T., Bryan, G. L. & Norman, M. L. 2003, ApJ, 587, 13 2003, (astro-ph/0312086)  
 Tonry, J. L. et al. 2001, ApJ, 546, 681  
 Tormen, G. 1997, MNRAS, 290, 411  
 Trentham, N., Tully, R. B. & Verheijen, M. A. W. 2001, MNRAS, 325, 385  
 Tully, R. B., Somerville, R. S., Trentham, N. & Verheijen, M. A. W. 2002, ApJ, 569, 573  
 Vader, J. P. & Sandage, A. 1991, ApJ, 379, L1  
 Wechsler, R. H., Bullock, J. S., Primack, J. R., Kravtsov, A. V. & Dekel, A. 2002, ApJ, 568, 52 Reed, D., & Quinn, T. 2004, MNRAS (submitted) (astro-ph/0403001)  
 Zhang, B., Wyse, R. F. G., Stiavelli, M. & Silk, J. 2002, MNRAS, 332, 647.

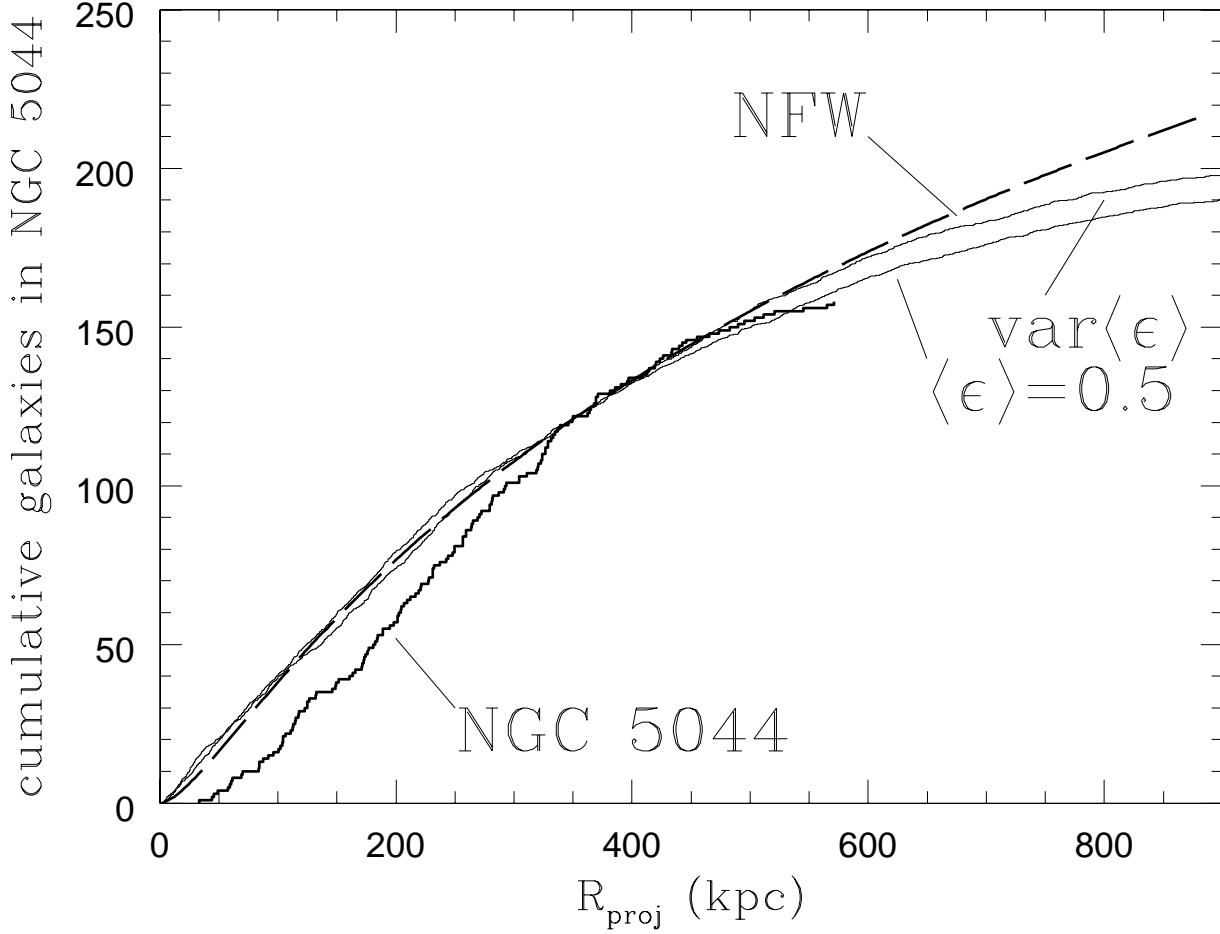


FIG. 1.— The irregular heavy line curve labeled “NGC 5044” is a cumulative histogram of the projected radii of low luminosity galaxies in the galaxy group NGC 5044. The heavy dashed line is the cumulative projected mass of an NFW profile normalized to agree with the NGC 5044 histogram at  $R = 350$  kpc. The two thin lines are dynamical models (actually histograms) of the cumulative radial distribution of dwarf galaxies in NGC 5044 if the galaxies entered the virialized halos in proportion to the dark matter. The circularity is constant for the  $\langle \epsilon \rangle = 0.5$  curve and increases with the virial mass from 0 to 1 in the curve labeled “var  $\langle \epsilon \rangle$ ”.

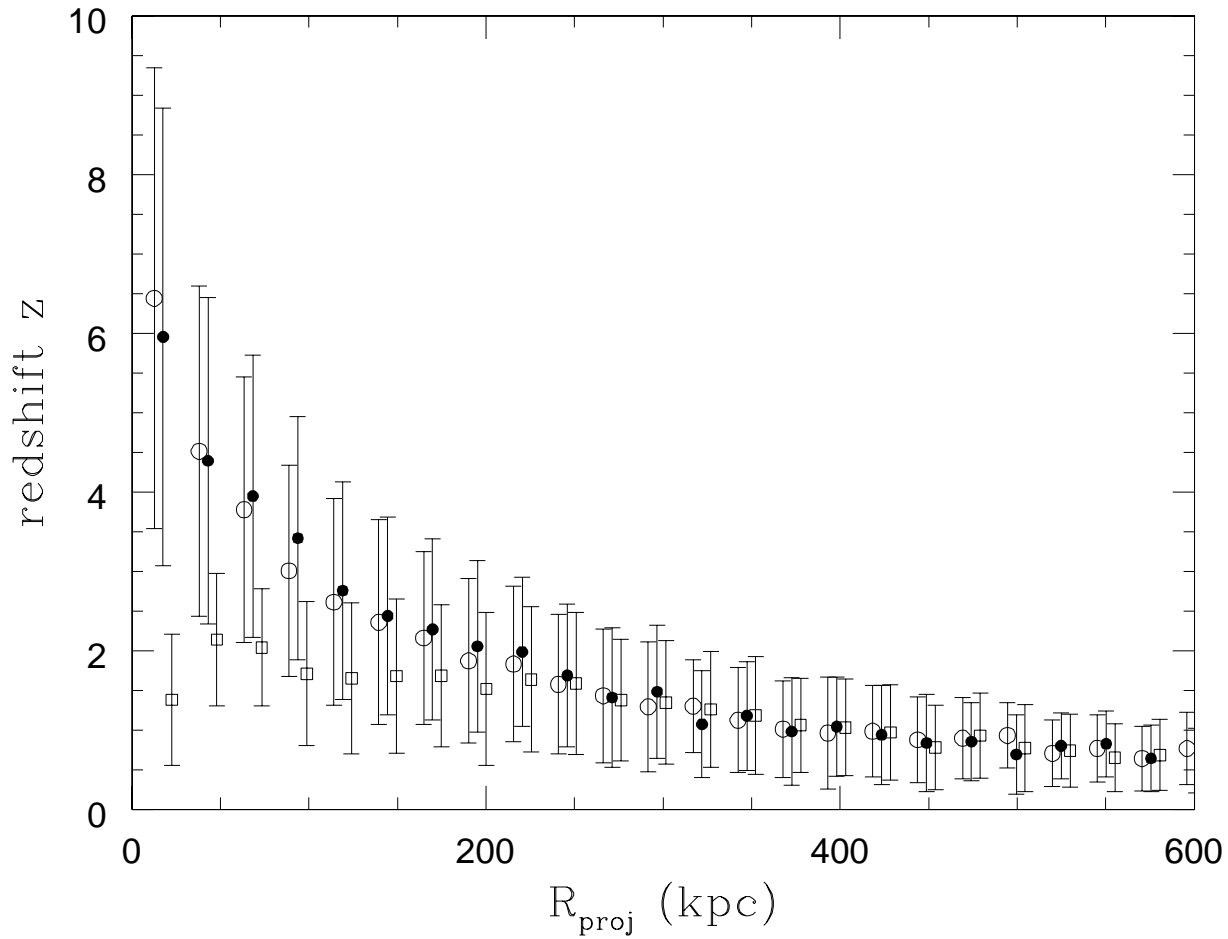


FIG. 2.— The mean redshift and redshift dispersion calculated for member galaxies in NGC 5044 in annular bins of projected radius. The open circles correspond to the  $\langle \epsilon \rangle = 0.5$  model in Figure 1. The filled circles and open squares correspond respectively to redshifts of model galaxies in models “var  $\langle \epsilon \rangle$ ” (Figure 1) and “ $z_c = 3.32, q = 0.1$ ” (Figure 4). All data points refer to the bins for the open circles but the filled circles and open squares have been shifted to the right for clarity.

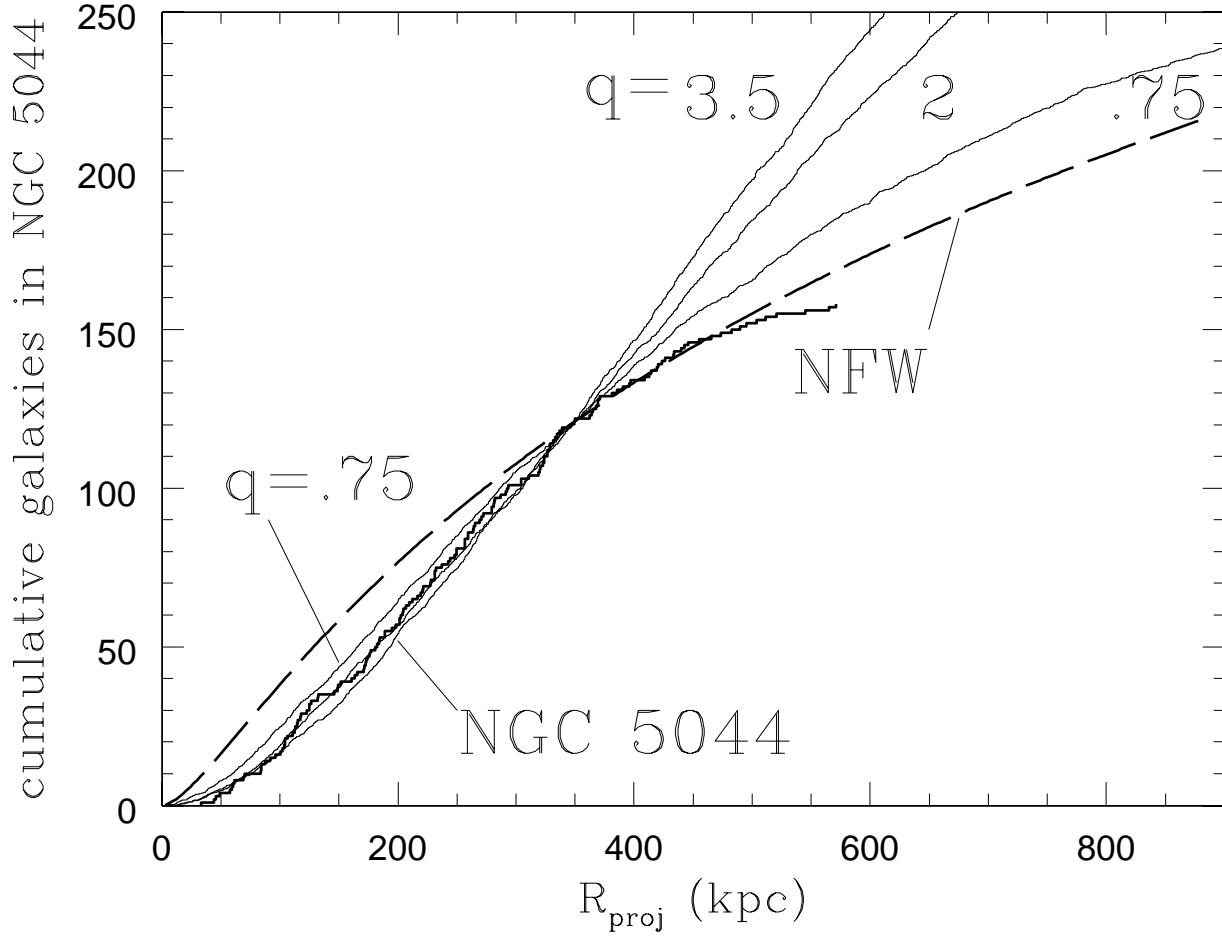


FIG. 3.— The observed histogram for NGC 5044 galaxies and the normalized NFW profile are identical to those in Figure 1. The three light lines are histograms of the cumulative number of galaxies in NGC 5044 assuming that they entered the virialized halo with probability density  $p'(M_v) \propto (M_v)^q$  with  $q = 0.75, 2$  and  $3.5$ .

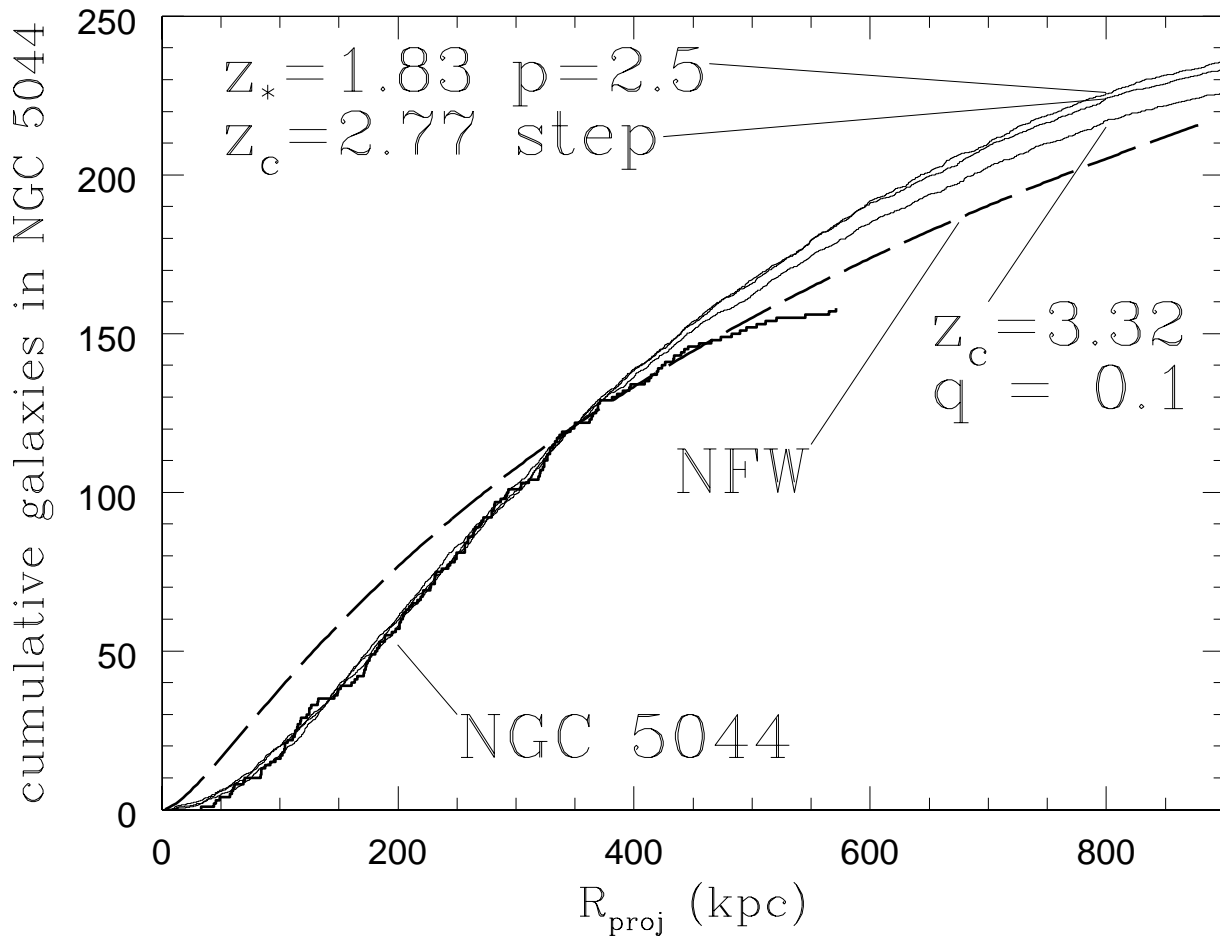


FIG. 4.— Three additional models for the entry and dynamics of dwarf galaxies in the NGC 5044 group. For the histogram labeled “ $z_c = 3.32$   $q = 0.1$ ” no galaxies entered the halo of the group before redshift 3.32 when the virial mass was  $M_c = 0.19M_{v,o}$ , but afterwards galaxies entered in proportion to  $(M_v - M_c)^{0.1}$ . The “ $z_c = 2.77$  step” curve shows the distribution of galaxies resulting from a step function at this redshift. In the galaxy distribution labeled “ $z_* = 1.83$   $p = 2.5$ ” galaxies entered the halo of NGC 5044 in as  $M_v^{2.5}$  until redshift  $z_* = 1.83$  and in proportion to the dark matter afterward. The observed histogram for NGC 5044 galaxies and the normalized NFW profile are identical to those in Figure 1.